Atmos. Chem. Phys. Discuss., 10, 4617–4647, 2010
www.atmos-chem-phys-discuss.net/10/4617/2010/

Atmospheric Chemistry and Physics Discussions

Structure-activity relationships to estimate the effective Henry's law coefficients of organics of atmospheric interest

T. Raventos-Duran[1], M. Camredon[1,*], R. Valorso[1], and B. Aumont[1]

[1]LISA, UMR CNRS/INSU 7583, Universités Paris 7 et Paris 12, 94010 Créteil Cedex, France
[*]now at: School of Geography, Earth & Environmental Science, University of Birmingham, Birmingham, B15 2TT, UK

Received: 19 January 2010 – Accepted: 8 February 2010 – Published: 16 February 2010

Correspondence to: B. Aumont (aumont@lisa.univ-paris12.fr)

Published by Copernicus Publications on behalf of the European Geosciences Union.

Abstract

The Henry's law coefficient is a key property needed to address the multiphase behaviour of organics in the atmosphere. Methods that can reliably predict the values for the vast number of organic compounds of atmospheric interest are therefore required. The effective Henry's law coefficient H^* in air-water systems at 298 K was compiled from literature for 488 organic compounds bearing functional groups of atmospheric relevance. This data set was used to assess the reliability of the HENRYWIN bond contribution method and the SPARC approach for the determination of H^*. Moreover, this data set was used to develop GROMHE, a new Structure Activity Relationship (SAR) based on a group contribution approach. These methods estimate $\log H^*$ with a Root Mean Square Error (RMSE) of 0.38, 0.61, and 0.73 log unit for GROMHE, SPARC and HENRYWIN respectively. The results show that for all these methods the reliability of the estimates decreases with increasing solubility. The main differences among these methods lie in H^* prediction for compounds with H^* greater than $10^3\,\mathrm{M\,atm^{-1}}$. For these compounds, the predicted values of $\log H^*$ using GROMHE are more accurate (RMSE=0.53) than the estimates from SPARC or HENRYWIN (RMSE=0.98 and 1.12).

1 Introduction

The oxidation of hydrocarbons emitted in the atmosphere involves complex reaction sequences. This oxidation is a gradual process leading to the formation of oxygenated organic intermediates usually denoted as secondary organics (e.g., Atkinson, 2000). The fate of these secondary organics remains poorly quantified due to a lack of information about their speciation, distribution and evolution in the gas and condensed phases (e.g., Goldstein and Galbally, 2007). Most secondary organics are expected to be water soluble, owing to the presence of polar moieties generated during the oxidation process. A significant fraction of secondary organics may thus dissolve into the tropospheric aqueous phase, namely rain, clouds and deliquescent particles (e.g., Saxena and Hildemann, 1996; Facchini et al., 1999). The resulting mass transfer is currently suggested to contribute to acid production, organic aerosol formation and the oxidant budget (e.g., Lelieveld and Crutzen, 1990; Walcek et al., 1997; Blando and Turpin, 2000; Ervens et al., 2003, 2008; Legrand et al., 2003, 2005; Yu et al., 2005; Gelencser and Varga, 2005; Lim et al., 2005; Hallquist et al., 2009).

In atmospheric models, the partitioning of organics between the gas and the aqueous atmospheric phases is usually described in the basis of Henry's law (e.g., Jacob et al., 1989; Aumont et al., 2000; Herrmann et al., 2000, 2005; Ervens et al., 2003, 2008; Pun et al., 2002; Griffin et al., 2003). Henry's law expresses the relationship between the solubility of a gas in a liquid and its partial pressure above that liquid: $S = H \times P$, where S is the solubility (M), P is the partial pressure (atm) and H is the Henry's law constant ($\mathrm{M\,atm^{-1}}$) at a given temperature. Henry's law is a limiting law that strictly applies to ideally dilute solutions. Atmospheric models require a knowledge of H for every water soluble organic species described in the chemical mechanism. Detailed gas phase or multiphase chemical mechanisms involve a vast number of species (e.g., Saunders et al., 2003; Aumont et al., 2005; Herrmann et al., 2005). The collection of Henry's law constants required to develop detailed models far exceeds the number of species for which experimental data is available. For example, the fully explicit oxidation mechanism developed by Camredon et al. (2007) for 1-octene includes 1.4×10^6 species and the gas/aerosol thermodynamic equilibrium for about 4×10^5 species. Reliable estimation methods for H are therefore required to design detailed mechanisms. To be useful, estimation methods must be applicable to a wide range of organics, especially to multifunctional species generated during the atmospheric oxidation of hydrocarbons. The aim of this paper is to identify a reliable method for estimating Henry's law constants for organic compounds of atmospheric interest in air-water systems.

Numerous structure activity relationships (SAR) have been developed to determine the Henry's law constant in a response to the difficulties associated with its laboratory measurement, in particular, for compounds with higher solubility (Mackay and Shiu,

1981; Russell et al., 1992; Hine and Mookerjee, 1975; Meylan and Howard, 1991; Suzuki et al., 1992). These SAR were reviewed and analysed by Dearden and Schuurmann (2003). This study showed that the bond contribution method developed by Meylan and Howard (1991) and updated in the frame of the HENRYWIN (HWINb) software (Meylan and Howard, 2000) was the most reliable method available. HWINb is based on the summation of the contributions of individual chemical bonds within compounds to determine the best fit of a multiple linear regression. Lin et al. (2002) pointed out that HWINb has a large number of descriptors with 64 bond contributions and 57 correction factors. A new method, SPARC, has been developed by Hilal et al. (2008). This method is based on the product of the activity coefficient in water γ_w^∞ and the vapour pressure P^o which are estimated using intermolecular interactions in the pure liquid phase and in solution. Hilal et al. (2008) used an experimental database of 1222 compounds for testing the air-to-water H. Their results show that for simple molecular structures, the standard deviation is within a factor of 2 but reaches a factor of 3 to 4 for more complex molecules having strong intramolecular and/or dipole-dipole interactions.

The objective of this paper is to assess the reliability of HWINb and SPARC methods. A experimental database of Henry's law constant was compiled for that purpose with special attention given to selecting those compounds with H above $10^3\,\mathrm{M\,atm^{-1}}$ which are soluble enough to have significant partitioning in the atmospheric aqueous phase (e.g., Seinfeld and Pandis, 1998; Gelencser and Varga, 2005). Furthermore, this database was used to develop a new GROup contribution Method for Henry's law Estimate (hereafter named GROMHE).

In this paper, we first describe the selection of the database used to develop and/or assess the estimation methods. We then describe the development of GROMHE and finally analyse the performance of the three methods considered for this study.

2 Database

Usually the experimental values found in the literature are expressed as effective Henry's law constants, H^*, which includes the hydration process. We differentiate the literature H^* values from the intrinsic H values as detailed in the next section. The database of Henry's law constants was compiled to include species representative of atmospheric oxidation processes occurring in the gas or aqueous phase. Table S1 (see the electronic supplement http://www.atmos-chem-phys-discuss.net/10/4617/2010/acpd-10-4617-2010-supplement.pdf) lists the experimental values selected in this study in units of $\mathrm{M\,atm^{-1}}$ and presented as the logarithm of H^*. The database includes 488 organic compounds comprising a wide range of functional groups detected in either gas or aqueous phase: nitrate, nitro, peroxyacylnitrate, aldehyde, ketone, ester, ether, alcohol, hydroperoxide, peracid, carboxylic acid and halogen (e.g., Finlayson-Pitts and Pitts, 2000; Seinfeld and Pandis, 1998). The number of species bearing a specific functional group is given in Table 1. The availability of data for hydroperoxide (3 species) and peracid (1 species) is limited and therefore it is difficult to assess the reliability of H^* estimates for these groups of species. The database is also poor for multifunctional oxygenated organics, although special care was taken to be as comprehensive as possible in the collection of experimental H^* for these groups of species. Data listed in Table S1 (http://www.atmos-chem-phys-discuss.net/10/4617/2010/acpd-10-4617-2010-supplement.pdf) includes H^* for 76 hydrocarbons, 231 monofunctional compounds, 132 difunctional compounds and 49 compounds bearing at least 3 functional groups. Both aliphatic and aromatic species were considered in the compilation and the data in Table S1 can be split into 393 aliphatic and 95 aromatic species. The constants included range from 10^{-4} to $10^{9}\,\mathrm{M\,atm^{-1}}$. Henry's law coefficients depend on the type of functional groups attached to the carbon chain and usually increase with the number of groups; for hydrocarbon species H^* ranges from 10^{-4} to $10^{-1}\,\mathrm{M\,atm^{-1}}$ whilst for monofunctional organic compounds H^* ranges from 10^{-1} to $10^{5}\,\mathrm{M\,atm^{-1}}$. Difunctionals compounds have the greatest range of H^*,

from 10^{-1} to $10^{9}\,\mathrm{M\,atm^{-1}}$.

Most of the Henry's law constants used in this study were collected from three different libraries; NIST (http://webbook.nist.gov/chemistry), the Sander data review (http://www.mpch-mainz.mpg.de/~sander/res/henry.html), and the Environment Protection Agency HENRYWIN program (Meylan and Howard, 2000) with a few additional values taken from recently published papers (see Table S1 in the electronic supplement). The data were exclusively taken from experimental values either from direct or indirect measurements. The indirect measurements are based on relationships between thermodynamic variables. In particular, for sparingly water soluble species, H^* is often estimated using the relationship: $H^* = S_w^s/P^o$ where S_w^s is the solubility for a saturated solution and P^o is the vapour above the pure compound in the condensed phase. Because S_w^s and P^o values are measured independently in the laboratory, we have two sources that contribute to the uncertainty in the final H^* value (Mackay and Shiu, 1981).

Most experimental H^* data in Table S1 are provided at 298 K. A small number of species measured at 293 K were also included to obtain a better representation of multifunctional oxygenated species. These values were corrected using the van't Hoff equation:

$$H_{298} = H_{293} \times \exp\left(\frac{\Delta \mathrm{H_{solv}}}{R}\left(\frac{1}{293} - \frac{1}{298}\right)\right) \tag{1}$$

where $\Delta\mathrm{H_{solv}}$ is the desolvation enthalpy and R is the gas constant. $\Delta\mathrm{H_{solv}}$ typically ranges from 10 to $100\,\mathrm{kJ\,mol^{-1}}$ (e.g., Kuhne et al., 2005) and a typical value of $50\,\mathrm{kJ\,mol^{-1}}$ was assumed here.

For empirically based methods, the experimental uncertainties are transferred into the models' uncertainties. However, uncertainties for the data reported in Table S1 (http://www.atmos-chem-phys-discuss.net/10/4617/2010/acpd-10-4617-2010-supplement.pdf) are hard to evaluate owing to the large number of experimental sources and the lack of reported experimental uncertainties in many of the original papers (Russell et al., 1992). During the compilation, we found that discrepancies in the measured H^* value for a given compound often exceeded a factor of 2. The discrepancies tend to increase with H^* which indicates the difficulties of measuring the physical property for those species with very high Henry's law constant (Hilal et al., 2008; Mackay and Shiu, 1981). As a guideline, we assume that the uncertainty is at least a factor of 2 for species having H^* above 10^5 M atm^{-1}.

3 Development of the GROMHE estimation method

3.1 Estimation method for hydration constants

Compounds containing carbonyl groups like aldehydes and ketones may undergo significant hydration. Carbonyls combine with water molecules to form gem diols upon dissolution according to the equilibrium:

$$> \mathrm{C{=}O} + \mathrm{H_2O} \longleftrightarrow > \mathrm{C(OH)(OH)}$$

The equilibrium of the carbonyls between the hydrated (> C(OH)(OH)) and non-hydrated (> C=O) form is described by the hydration constant K_{hyd}:

$$K_{\mathrm{hyd}} = \frac{[> \mathrm{C(OH)(OH)}]}{[> \mathrm{C{=}O}]} \tag{2}$$

Table S2 (see the electronic supplement http://www.atmos-chem-phys-discuss.net/10/4617/2010/acpd-10-4617-2010-supplement.pdf) shows the compilation of the hydration constants for 61 aldehydes and/or ketones. K_{hyd} is typically about 10^{-3} and 1 for simple ketones and aldehydes, respectively. K_{hyd} increases by 1 to 3 orders of magnitude when a strongly polar group is attached to the carbon next to the carbonyl group. Hydration is therefore a key parameter affecting the solubility of multifunctional carbonyl compounds.

The partitioning of species that undergo hydration in water is usually described with the effective Henry's law constant H^*. The effective Henry's law constant of a compound is defined as the ratio between the total dissolved concentration and its pressure:

$$H^* = \frac{([> \mathrm{C{=}O}] + [> \mathrm{C(OH)(OH)}])}{P_{>\mathrm{C{=}O}}} = H\left(1 + K_{\mathrm{hyd}}\right) \tag{3}$$

where H is the intrinsic Henry's law coefficient for the carbonyl. The values extracted from the literature and listed in Table S1 (see the electronic supplement http://www.atmos-chem-phys-discuss.net/10/4617/2010/acpd-10-4617-2010-supplement.pdf) are therefore H^* for carbonyls.

Most estimation methods were based on group contribution methods using $\log H^*$ as the training data set. Equation (3) shows that for carbonyls, H^* is a function of 2 fundamental properties (H and K_{hyd}). If $K_{\mathrm{hyd}} \gg 1$ then $\log H^* \approx \log H + \log K_{\mathrm{hyd}}$. On the other hand, if $K_{\mathrm{hyd}} \ll 1$, then $\log H^* \approx \log H$. This conditional addition of $\log K_{\mathrm{hyd}}$ is hard to represent by a simple group contribution method which assumes additive groups. Here we estimated both K_{hyd} and the intrinsic H for each carbonyl and used Eq. (3) to finally compute H^*. Note that the method performance was assessed on the accuracy of H^* which is the primary property being investigated.

A multiple linear regression was performed using the data shown in Table S2 (http://www.atmos-chem-phys-discuss.net/10/4617/2010/acpd-10-4617-2010-supplement.pdf) as a training set. K_{hyd} has been found to be well correlated with the inductive effect of the neighbouring groups (Le Henaff, 1968; Betterton and Hoffmann, 1988). Taft and Hammett σ were used as descriptors for aliphatic and aromatic compounds, respectively (see Table 2). Hammett values for the various functional groups were obtained from the data reviews of Hansch et al. (1995) and Perrin et al. (1981). We defined a "Hammett descriptor" (referenced as hdescriptor in Table 3) as the sum of the contribution of each group:

$$\mathrm{hdescriptor} = \Sigma\sigma_o + \Sigma\sigma_m + \Sigma\sigma_p \tag{4}$$

where σ_o, σ_m, σ_p are the Hammett sigma values for the functional groups in ortho, meta or para positions relative to the benzaldehyde group (see Table 2). Similarly, we defined a "Taft descriptor" (tdescriptor) as:

$$\text{tdescriptor} = \Sigma\sigma_i^* \tag{5}$$

where σ_i^* are the Taft sigma values for the functional groups i borne by the molecule in relation to the carbonyl group (see Table 2). Two additional molecular descriptors were introduced to discriminate aromatic from aliphatic compounds and ketone from aldehyde groups. Table 3 provides the optimised weight for these 4 descriptors and Fig. 1 shows the resulting scatter plot. The coefficient of determination is $R^2 = 0.90$. The reliability of the method was assessed using the root mean square error (RMSE) defined as:

$$\text{RMSE} = \sqrt{\frac{1}{n}\sum_{i=1}^{n}\left(\log K_{\text{hyd,est}} - \log K_{\text{hyd,exp}}\right)^2} \tag{6}$$

The RMSE obtained is 0.47 log unit. The method allows estimating K_{hyd} within a factor of 3.

3.2 Estimation method for the intrinsic Henry's law constants

The GROMHE approach is similar to the method described by Suzuki et al. (1992) and is based on considering a molecule as a collection of elemental constituents (functional groups or atoms) whose contributions are computed using a multiple linear regression (MLR). The original approach by Suzuki et al. (1992) was developed for monofunctional species only. In GROMHE, the approach is extended to multifunctional species using additional descriptors to account for group interactions. The identification of descriptors is complex and requires compromises between the quality of the linear regression and the prediction ability of the parametric relations, which decreases when increasing the number of descriptors, in an opposite way to the quality. An attempt was made to

minimise the number of descriptors and to optimise the regression for the species of atmospheric interest.

The database was split into two sets: 70% of the data were used as training set and the remaining 30% were reserved for validation and were not used during the development of the method. The training data set was then used to compute the contribution of the descriptors selected for the regression. Species used for validation were randomly selected and are given in Table S1 (see the electronic supplement http://www.atmos-chem-phys-discuss.net/10/4617/2010/acpd-10-4617-2010-supplement.pdf). This random selection covered structurally diverse compounds representative of all type of functional groups included in the database (see Table 1). The effective Henry's law constants collected in our data set were corrected for hydration to determine intrinsic values. The structure activity relationship (SAR) presented in the previous section was used systematically to derive the hydration constants for ketones and aldehydes and to compute the intrinsic Henry's law constant (H) values. These derived intrinsic H values were used as the training data set for the MLR analysis. Our model uses 28 independent descriptors, presented below. The list of descriptors along with their weight in the regression and standard errors are shown in Table 1.

Suzuki et al. (1992) have shown that H can be estimated for hydrocarbons and monofunctional species using the organic functionalities as descriptors along with the number of carbon and hydrogen atoms. We introduced 16 descriptors, each corresponding to a distinct organic functionality identified within the compounds comprising the study data set (see Table 1), and two structural descriptors to account for the number of hydrogen and carbon atoms.

In contrast to Suzuki et al. (1992) who duplicated the descriptors to differentiate functionalities bound to an aromatic chain from those bound to an aliphatic chain, we simply defined two additional descriptors to account for the number of groups bound to an aromatic ring or an olefinic carbon respectively, so as to keep the number of descriptors to a minimum. These descriptors are referenced as nfcd and nfaro in Table 1. An MLR using these 20 structural descriptors was able to provide H estimates with an R^2 of 0.97 for the hydrocarbons and monofunctional species included in the data set.

Extrapolation of our model using the 20 descriptors defined above however leads to errors in the estimated values exceeding 3 orders of magnitude for some difunctional species. Additional descriptors were therefore included to account for intramolecular group interactions. The mutual inductive effect between functional groups was explored as a parameter linked to the overestimation of H^* identified in multifunctional species. Here, we introduced Sigma Taft (σ^*) as a descriptor for aliphatic species (e.g., Hansch et al., 1995). Group interactions were taken into account by adding, for each group i, the σ_j^* of the neighbouring group j:

$$\text{tdescriptor} = \sum_i \sum_{j \neq i} \sigma_j^* \tag{7}$$

where tdescriptor is the parameter used as a descriptor for the regression. Values for σ_j^* are provided in Table 2 for each of the 16 functional groups encountered in the database. tdescriptor was found to be statistically significant for the prediction of H at the 99.9% confidence level (see p-value in Table 1). The inclusion of tdescriptor in the set of descriptors leads to a fairly good estimate of H for multifunctional compounds bearing nitro, nitrate and/or halogen groups. However, H was still overestimated for multifunctional species bearing carbonyl or hydroxyl moieties, so additional descriptors were introduced.

Scatter plots showed that species with a $-\mathrm{C(=O)-C(X)}<$ structure where X is an oxygenated moiety (carbonyl, alcohol, ether, hydroperoxide or nitro) have lower H values than predicted by simple group addition. A specific structural descriptor (caox-a in Table 1) was therefore introduced to account for this effect. A similar trend was also observed when the X moiety was located in the β position relative to the carbonyl group and was accounted for by the inclusion of the caox-b descriptor. Similarly, H was found to be overestimated for species having a functional group in the α or β position relative to an alcohol moiety. This effect might be linked to some intramolecular H-bonding

(e.g., Hine and Mookerjee, 1975; Hilal et al., 2008). This effect was taken into account with the help of two additional structural descriptors: hyd-a and hyd-b. The inclusion of these 4 descriptors was found to greatly improve H estimates for the multifunctional oxygenated species. However, a bias in predicted H was still found for 2 groups of species: o-nitrophenols and halogenated species bearing a carboxylic acid moiety in the α position. Two additional descriptors (haloic-a, onitrofol in Table 1) were introduced to correct this bias. This is similar to the correction factors applied in the QSAR method developed by Russell et al. (1992) and in the HENRYWIN method.

The 27 descriptors listed above were all found to be significant for the prediction of H at the 99.9% confidence level (see the p-values in Table 1). However, a small bias was observed in the prediction of H for hydrocarbons and a final descriptor (nogrp in Table 1) was included to correct this bias. The computed weight for nogrp remains low and this factor is the least significant in the regression (see the p-value in Table 1).

Figure 2 shows the performance of GROMHE. The scatter plot for the training set in Fig. 2 shows that one species, oxo-acetic acid, behaves as an outlier with $\log H^*$ overestimated by 3 log unit. This species was found to be overestimated by 6 log unit using SPARC (see below). The reason of this large overestimation remains unresolved to us and we decided to remove that species from the GROMHE optimisation training set. For the purpose of the intercomparison, oxo-acetic acid was also removed from the statistical analysis. The reliability of the predictions were assessed using the Root Mean Square Error (RMSE), determined as described previously in the context of the hydration constant assessment (see Eq. 6), the Mean Absolute Error (MAE) and the Mean Bias Error (MBE):

$$\text{MAE} = \frac{1}{n} \sum_{i=1}^{n} \left| \log H^*_{\text{est}} - \log H^*_{\text{exp}} \right| \tag{8}$$

$$\text{MBE} = \frac{1}{n} \sum_{i=1}^{n} \left(\log H^*_{\text{est}} - \log H^*_{\text{exp}} \right) \tag{9}$$

The MAE, MBE and RMSE are given in Fig. 2 for the training and validation data sets. Figure 2 shows that the model explains 97% of the total variance of the validation data set. Estimated logH^* values for the validation set shows no significant bias (MBE=0.04). The RMSE for the validation set is 0.39, which corresponds to an estimation ability of H^* within a factor of 2.5. The RMSE, MAE, MBE and R^2 values for the validation set are similar to those calculated for the training set and show that the model is not over-fitted (see Fig. 2).

3.3 Analysis of GROMHE estimation method

The previous section shows that GROMHE provides reliable estimates of H^*. The contribution of the descriptors was optimised to obtain a more representative model using the full database. These final contributions agree with those computed for the training data set within their statistical uncertainties (see Table 1). The analysis of GROMHE predictions were performed using the optimised weights.

The overall performance of GROMHE is summarised in the scatter plot shown in Fig. 3. The RMSE, MAE and MBE are shown in Fig. 4 together with the box plot of error distribution. The assessment was also performed for different subsets to identify possible bias for various groups of species. Three categories of subsets were defined according to: (1) the number of functional groups (hydrocarbons, monofunctional, difunctional and multifunctional), (2) the aromatic or aliphatic structure of the molecule and (3) the range of the Henry's law constant to differentiate fairly insoluble species (with H^* below 10^3 M atm^{-1}) from more soluble species (H^* greater than 10^3 M atm^{-1}).

The coefficient of determination R^2 between experimental and predicted logH^* is 0.97 (see Fig. 3). No significant MBE was found for any of the subsets (see Fig. 4) and thus the GROMHE method seems to provide no systematic bias. Box and scatter plots show that the error increases from simple hydrocarbons to multifunctional species. The RMSE is 0.30 for hydrocarbons and reaches a maximum of 0.52 for difunctional species (see Fig. 4). Similarly, the error in predicting logH^* for more soluble compounds (i.e. more oxygen substituted compounds) is significantly greater than for less soluble

species. The RMSE is 0.33 and 0.53 for the subset of species having H^* below and above 10^3 M atm^{-1}, respectively. It was also observed that the method provides better estimates for the aliphatic subset of species compared to the aromatic subset (see Fig. 4). For the full database, GROMHE finally gives fairly reliable logH^* estimates, with RMSE of 0.38 and MAE of 0.27.

4 Analysis of HWINb and SPARC estimation methods

HWINb, SPARC methods are able to estimate H^* for all the species selected in the database (see Table S1 in the electronic supplement http://www.atmos-chem-phys-discuss.net/10/4617/2010/acpd-10-4617-2010-supplement.pdf). H^* estimates from HWINb method were determined using the software EPIWIN suit (http://www.epa.gov/oppt/exposure/pubs/episuitedl.htm). The SPARC calculator (http://sparc.chem.uga.edu/sparc) estimates independently the intrinsic H and the hydration constant K_{hyd}. These two properties were jointly used to retrieve the effective Henry's law coefficient H^* from Eq. (3). The values reported in Table S1 refer to the retrieved logH^*. The overall performance of the models HWINb and SPARC are summarised in scatter plots (Figs. 5 and 6). The RMSE, MAE and MBE for each method are shown in Figs. 7 and 8 together with the box plot of error distribution.

For the method HWINb, the scatter plot is shown in Fig. 5 and the performance in Fig. 7. The coefficient of determination for logH^*_{est} versus logH^*_{exp} is $R^2 = 0.91$. Hydrocarbon and monofunctional compounds are well predicted with a performance similar to GROMHE's performance. However, their prediction error is much larger for multifunctional compounds with RMSE above 1.0 log unit (see Fig. 7). A bias was also found with a slight tendency towards overestimation of logH^* for difunctional species and underestimation for species having more than 2 functional groups. This prediction error shows a behaviour similar to that seen for GROMHE, i.e. the error grows with increasing solubility. For the subset of species H^* above 10^3 M atm^{-1}, the RMSE reaches 1.1 log unit which is twice the RMSE given by the GROMHE method. Furthermore, the error obtained with GROMHE for each subset is systematically lower than those obtained using HWINb.

The correlation logH^* estimated using SPARC versus experimental logH^* is shown in Fig. 6. The coefficient of determination R^2 is 0.94. SPARC performance is shown in Fig. 8. SPARC and HWINb show similar reliability with similar trends in the prediction of logH^* for the various subsets. Hydrocarbons and monofunctional compounds are well represented (RMSE < 0.5) whilst errors become large for multifunctional species (RMSE $= 0.97$). Similar to HWINb results, a bias towards logH^* overestimation is found for difunctional species and towards underestimation for tri or more functional species. Like GROMHE and HWINb the reliability of SPARC estimates decreases with increasing solubility. The error is about one order of magnitude for species having H^* above 10^3 M atm^{-1} (see Fig. 8).

5 Conclusions

A new group contribution method, GROMHE, was developed in this study to estimate H^* for organic compounds at 298 K. A multiple linear regression was performed using the training data set including 345 organics representative species of atmospheric interest. A set of 28 descriptors was found to be statistically significant for the prediction of logH^*. The resulting method predicts logH^* with a root mean square error of 0.39 for a validation set including 142 species. No statistically significant bias was observed. The regression fit of predicted versus observed logH^* show a coefficient of determination of $R^2 = 0.97$.

The results of estimating H^* using the HWINb and SPARC with the data set compiled here show a tendency towards underestimation for compounds with two functional groups and overestimation for compounds with more than two. However, H^* values for hydrocarbon and monofunctional compounds were well predicted using any of the methods assessed, with similar performance. All methods show that the reliability of the predicted values decreases when H^* increases. Species having H^* above

10^3 M atm^{-1} are of particular interest in the context of atmospheric chemistry. For the subset of species having H^* above that threshold, the RMSE obtained for GROMHE is 0.53 log unit. For the same subset, the reliability of the prediction using HWINb or SPARC was appreciably lower with RMSE of about 1 log unit. This best agreement must however be weighted since GROMHE was specifically designed and adjusted for the database selected here. Additional work would be required to evaluate the inherent performance of the HWINb method by optimising the bond contributions for the same database as used here before reaching any final conclusions.

Acknowledgements. We would like to thank S. H. Hilal and L. A. Carreira for providing us with data and support to run SPARC. Helpful comments on the manuscript by A. Dutot and J. Lee-Taylor are gratefully acknowledged.

The publication of this article is financed by CNRS-INSU.

References

Atkinson, R.: Atmospheric chemistry of VOCs and NO_x, Atmos. Environ., 34, 2063–2101, 2000. 4618

Aumont, B., Madronich, S., Bey, I., and Tyndall, G. S.: Contribution of secondary VOC to the composition of aqueous atmospheric particles: a modeling approach, J. Atmos. Chem., 35, 59–75, 2000. 4619

Aumont, B., Szopa, S., and Madronich, S.: Modelling the evolution of organic carbon during its gas-phase tropospheric oxidation: development of an explicit model based on a self generating approach, Atmos. Chem. Phys., 5, 2497–2517, 2005, http://www.atmos-chem-phys.net/5/2497/2005/. 4619

Betterton, E. A. and Hoffmann, M. R.: Henry's law constants of some environmentally important aldehydes, Environ. Sci. Technol, 22, 1415–1418, 1988. 4624

Blando, J. D. and Turpin, B. J.: Secondary organic aerosol formation in cloud and fog droplets: a literature evaluation of plausibility, Atmos. Environ., 34, 1623–1632, 2000. 4619

Camredon, M., Aumont, B., Lee-Taylor, J., and Madronich, S.: The SOA/VOC/NO_x system: an explicit model of secondary organic aerosol formation, Atmos. Chem. Phys., 7, 5599–5610, 2007, http://www.atmos-chem-phys.net/7/5599/2007/. 4619

Chen, J., Griffin, R. J., Grini, A., and Tulet, P.: Modeling secondary organic aerosol formation through cloud processing of organic compounds, Atmos. Chem. Phys., 7, 5343–5355, 2007, http://www.atmos-chem-phys.net/7/5343/2007/.

Dearden, J. C. and Schuurmann, G.: Quantitative structure-property relationships for predicting Henry's law constant from molecular structure, Environ. Toxicol. Chem., 22, 1755–1770, 2003. 4620

Ervens, B., George, C., Williams, J. E., Buxton, G. V., Salmon, G. A., Bydder, M., Wilkinson, F., Dentener, F., Wolke, R., and Herrmann, H.: CAPRAM 2.4 (MODAC mechanism): an extended and condensed tropospheric aqueous phase mechanism and its application, J. Geophys. Res.-Atmos., 108, 4426, doi:4410.1029/2002JD002202, 2003. 4619

Ervens, B., Carlton, A. G., Turpin, B. J., Altieri, K. E., Kreidenweis, S. M., and Feingold, G.: Secondary organic aerosol yields from cloud-processing of isoprene oxidation products, Geophys. Res. Lett., 35(5), L02816, doi:10.1029/2007JL031828, 2008. 4619

Facchini, M. C., Fuzzi, S., Zappoli, S., Andracchio, A., Gelencser, A., Kiss, G., Krivacsy, Z., Meszaros, E., Hansson, H. C., Alsberg, T., and Zebuhr, Y.: Partitioning of the organic aerosol component between fog droplets and interstitial air, J. Geophys. Res.-Atmos., 104, 26821–26832, 1999. 4619

Finlayson-Pitts, B. J. and Pitts, J. N.: Chemistry of the upper and lower atmosphere, Academic Press, San Diego, 2000. 4621

Gelencsér, A. and Varga, Z.: Evaluation of the atmospheric significance of multiphase reactions in atmospheric secondary organic aerosol formation, Atmos. Chem. Phys., 5, 2823–2831, 2005, http://www.atmos-chem-phys.net/5/2823/2005/. 4619, 4620

Goldstein, A. H. and Galbally, I. E.: Known and unexplored organic constituents in the earth's atmosphere, Environ. Sci. Technol., 41, 1514–1521, 2007. 4618

Griffin, R. J., Nguyen, K., Dabdub, D., and Seinfeld, J. H.: A coupled hydrophobic-hydrophilic model for predicting secondary organic aerosol formation, J. Atmos. Chem., 44, 171–190, 2003. 4619

Hallquist, M., Wenger, J. C., Baltensperger, U., Rudich, Y., Simpson, D., Claeys, M., Dommen, J., Donahue, N. M., George, C., Goldstein, A. H., Hamilton, J. F., Herrmann, H., Hoffmann, T., Iinuma, Y., Jang, M., Jenkin, M. E., Jimenez, J. L., Kiendler-Scharr, A., Maenhaut, W., McFiggans, G., Mentel, Th. F., Monod, A., Prvt, A. S. H., Seinfeld, J. H., Surratt, J. D., Szmigielski, R., and Wildt, J.: The formation, properties and impact of secondary organic aerosol: current and emerging issues, Atmos. Chem. Phys., 9, 5155–5236, 2009, http://www.atmos-chem-phys.net/9/5155/2009/. 4619

Hansch, C., Leo, A., and Hoekman, D.: Exploring QSAR: Hydrophobic, Electronic, and Steric Constants. American Chemical Society, Washington D.C., 1995. 4624, 4627

Herrmann, H., Ervens, B., Jacobi, H.-W., Wolke, R., Nowacki, P., and Zellner, R.: CAPRAM2.3: A chemical aqueous phase radical mechanism for tropospheric chemistry, J. Atmos. Chem., 36, 231–284, 2000. 4619

Herrmann, H., Tilgner, A., Barzaghi, P., Majdik, Z., Gligorovski, S., Poulain, L., and Monod, A.: Towards a more detailed description of tropospheric aqueous phase organic chemistry: CAPRAM 3.0, Atmos. Environ., 39, 4351–4363, 2005. 4619

Hilal S. H., Ayyampalayam S. N., and Carreira, L. A.: Air-liquid partition coefficient for a diverse set of organic compounds: Henry's law constant in water and hexadecane, Environ. Sci. Technol., 42(24), 9231–9236, 2008. 4620, 4623, 4628

Hine, J. and Moorkerjee, P. K.: The intrinsic hydrophilic character of organic compounds. Correlations in terms of structural contributions, J. Org. Chem., 40, 292–298, 1975. 4620, 4628

Jacob, D., Gottlieb, E. W., and Prather, M. J.: Chemistry of polluted cloudy boundary layer, J. Geophys. Res.-Atmos., 94, 12975–13002, 1989. 4619

Kuhne, R., Ebert, R. U., and Schuurmann, G.: Prediction of the temperature dependency of Henry's law constant from chemical structure, Environ. Sci. Technol., 39(17), 6705–6711, 2005. 4622

Le Henaff, P.: Methodes d'etude et proprietes des hydrates, hemiacetals et hemithioacetals derives des aldehydes et des cetones, P. Bull. Soc. Chim. Fr., 11, 4687–4698, 1968. 4624

Legrand, M., Preunkert, S., Wagenbach, D., Cachier, H., and Puxbaum, H.: A historical record of formate and acetate from a high-elevation alpine glacier: Implications for their natural versus anthropogenic budgets at the European scale, J. Geophys. Res.-Atmos., 108(15), 4788, doi:10.1029/2003JD003594, 2003. 4619

Legrand, M., Preunkert, S., Galy-Lacaux, C., Liousse, C., and Wagenbach, D.: Atmospheric year-round records of dicarboxylic acids and sulfate at three French sites located between 630 and 4360 m elevation, J. Geophys. Res., 110, D13302, doi:10.1029/2004JD005515, 2005. 4619

Lelieveld, J. and Crutzen, P. J.: Influences of cloud photochemical processes on tropospheric ozone, Nature, 343, 227–233, 1990. 4619

Lim, H. J., Carlton, A. G., and Turpin, B. J.: Isoprene forms secondary organic aerosol through cloud processing: Model simulations, Environ. Sci. Technol., 39(12), 4441–4446, 2005. 4619

Lin, S. T. and Sandler, S. I.: Henry's law constant of organic compounds in water from a group contribution model with multipole corrections, Chem. Eng. Sci., 57, 2727–2733, 2002. 4620

Mackay, D. and Shiu, W. Y.: A critical-review of Henrys law constants for chemicals of environmental interest, J. Phys. Chem. Ref. Data., 10, 1175–1199, 1981. 4619, 4622, 4623

Meylan, W. M. and Howard, P. H.: Bond contribution method for estimating Henry's law constants, Environ. Toxicol. Chem, 10, 1283–1293, 1991. 4620

Meylan, W. M. and Howard, P. H.: Src's epi suite, v3.20, Syracuse Research Corporation: Syracuse. NY, 2000. 4620, 4622

Perrin, D. D., Dempsey, B., and Serjeant, E. P.: pKa prediction for organic acids and bases, Chapman and Hall, London and New York, 1981. 4624

Pun, B. K., Griffin, R. J., Seigneur, C., and Seinfeld, J. H.: Secondary organic aerosol-2. Thermodynamic model for gas/particule partitioning of molecular constituents, J. Geophys. Res., 107(D17), 4333, doi:10.1029/2001JD000542, 2002. 4619

Russell, C. J., Dixon, S. L., and Jurs, P. C.: Computer-assisted study of the relationship between molecular-structure and Henry Law constant, Anal. Chem., 64, 1350–1355, 1992. 4620, 4623, 4628

Sander, R.: Compilation of Henry's law constants for inorganic and organic species of potential importance in environmental chemistry (Version 3): www.henrys-law.org, 1999.

Saunders, S. M., Jenkin, M. E., Derwent, R. G., and Pilling, M. J.: Protocol for the development of the Master Chemical Mechanism, MCM v3 (Part A): tropospheric degradation of non-aromatic volatile organic compounds, Atmos. Chem. Phys., 3, 161–180, 2003, http://www.atmos-chem-phys.net/3/161/2003/. 4619

Saxena, P. and Hildemann, L. M.: Water-soluble organics in atmospheric particles: a critical review of the literature and application of thermodynamics to identify candidate compounds, J. Atmos. Chem., 24, 57–109, 1996. 4619

Seinfeld, J. H. and Pandis, S. N.: Atmospheric chemistry and physics, Wiley, New York, 1998. 4620, 4621

Suzuki, T., Ohtaguchi, K., and Koide, K.: Application of principal components-analysis to calculate Henry constant from molecular-structure, Comput. Chem., 16, 41–52, 1992. 4620, 4625, 4626

Walcek, C. J., Yuan, H. H., and Stockwell, W. R.: The influence of aqueous-phase chemical reactions on ozone formation in polluted and nonpolluted clouds, Atmos. Environ., 31, 1221–1237, 1997. 4619

Yu, L. E., Shulman, M. L., Kopperud, R., and Hildemann, L. M.: Characterization of organic compounds collected during southeastern aerosol and visibility study: Water-soluble organic species, Environ. Sci. Technol., 39(3), 707–715, 2005. 4619

Table 1. Descriptors for the model GROMHE, number of species in the database contributing to the descriptor and their related contribution, standard error and statistical significance in the MLR.

Descriptor[a]	Training dataset				All dataset			
	Number of species	Contribution	Standard Error	P-Value	Number of species	Contribution	Standard Error	P-Value
Functional group and structural descriptors								
# of hydroxy groups (–OH)	85	4.56	0.11	0.0000	120	4.56	0.09	0.0000
# of nitro groups (–NO_2)	22	3.06	0.12	0.0000	27	3.02	0.10	0.0000
# of nitrate groups (–ONO_2)	33	2.06	0.07	0.0000	44	2.04	0.06	0.0000
# of hydroperoxide groups (–OOH)	1	4.98	0.42	0.0000	3	4.87	0.24	0.0000
# of fluorine groups (–F)	15	0.60	0.10	0.0000	19	0.60	0.08	0.0000
# of chlorine groups (–Cl)	26	0.88	0.07	0.0000	51	0.87	0.06	0.0000
# of bromine groups (–Br)	15	1.04	0.10	0.0000	21	1.06	0.09	0.0000
# of iodine groups (–I)	7	1.15	0.18	0.0000	11	1.22	0.13	0.0000
# of aldehyde groups (–CHO)	18	2.63	0.12	0.0000	24	2.59	0.11	0.0000
# of ketone groups (–COR)	22	3.29	0.12	0.0000	35	3.16	0.10	0.0000
# of acid groups (–COOH)	27	5.11	0.11	0.0000	36	5.09	0.09	0.0000
# of peracid groups (–COOOH)	1	4.68	0.41	0.0000	1	4.68	0.40	0.0000
# of peroxyacyl nitrate groups (–PAN)	3	1.94	0.25	0.0000	5	1.93	0.19	0.0000
# of ether groups (–OR)	42	2.44	0.10	0.0000	52	2.40	0.09	0.0000
# of ester groups (–COOR)	37	2.79	0.10	0.0000	55	2.78	0.08	0.0000
# of formate groups (–HCOOR)	3	2.39	0.25	0.0000	4	2.36	0.21	0.0000
# of C atoms	345	0.49	0.02	0.0000	488	0.50	0.02	0.0000
# of H atoms	345	–0.31	0.01	0.0000	488	–0.31	0.01	0.0000
nfcd	26	–0.59	0.07	0.0000	37	–0.52	0.05	0.0000
nfaro	48	–1.10	0.07	0.0000	67	–1.12	0.06	0.0000
Group interaction descriptors								
tdescriptor	98	–0.14	0.01	0.0000	138	–0.14	0.01	0.0000
caox–a	9	–1.78	0.17	0.0000	13	–1.77	0.13	0.0000
caox–b	8	–1.31	0.18	0.0000	12	–1.09	0.14	0.0000
hyd–a	18	–0.63	0.13	0.0000	29	–0.60	0.10	0.0000
hyd–b	15	–1.00	0.18	0.0000	23	–1.03	0.14	0.0000
Correction factor descriptors								
haloic–a	5	0.98	0.21	0.0000	10	0.97	0.15	0.0000
onitrofol	7	–2.72	0.23	0.0000	10	–2.66	0.19	0.0000
nogrp	52	–0.31	0.11	0.0069	76	–0.28	0.09	0.0028
Intercept	–	–1.51	0.11	0.0000	–	–1.52	0.09	0.0000

[a] See text for the meaning of the descriptor.

Table 2. Sigma Taft and Hammett values for organic functional groups (adapted from Perrin et al., 1981).

Functional group	Taft σ^{*a}	Hammett ortho σ_o	Hammett meta σ_m	Hammett para σ_p
ROH	0.62	0.13	–0.38	1.22
RNO_2	1.47	0.74	0.78	1.99
$RONO_2^b$	1.52	0.55	0.7	–
ROOH [c]	0.62	–	–	–
RF	1.10	0.34	0.06	0.93
RCl	0.94	0.37	0.24	1.28
RBr	1.00	0.39	0.22	1.35
RI	1.00	0.35	0.21	1.34
RCHO	2.15	0.36	0.44	0.36
RCOR	1.81	0.36	0.47	0.07
RCOOH	2.08	0.35	0.44	0.95
COOOH[c]	2.08	–	–	–
PAN[c]	2.00	–	–	–
ROR	1.81	0.11	–0.28	0.12
ROCOR[d]	2.56	0.32	0.39	0.63
RCOOR[e]	2.00	0.32	0.39	0.63
HCOOR	2.90	–	–	–

[a] Reported σ^* is the inductive effect that the carbon bearing the functional group exerts on its direct neighbouring groups. According to Perrin et al. (1981) σ^* for functional groups attached to carbons at distant positions are determined as $\sigma = \sigma_i \times (0.4)^n$ where n is the number of aliphatic carbons separating the functional groups. The 2 carbons forming a C=C bond are counted as one C only. [b] Perrin et al. (1981) gives σ^* =3.86 for the nitrate group. The value reported here is $\sigma^* = 0.4 \times 3.86$, estimated for the carbon bearing the nitrate functional group to its neighbouring groups. [c] Value set assuming that $\sigma_{ROOH} = \sigma_{ROH}$, $\sigma_{C(O)OOH} = \sigma_{RC(O)OH}$, $\sigma_{PAN} = \sigma_{RCOOCH3}$.
[d] Sigma for ester at the -O- side. [e] Sigma for ester at the -CO side.

Table 3. Descriptors for the model to estimate hydration constants and their related contribution, standard error and statistical significance (p-value) in the MLR.

Descriptor	Contribution	Standard Error	p-Value
tdescriptor[a]	1.27	0.07	0.0000
hdescriptor[a]	0.50	0.17	0.0049
Ketone flag[b]	−2.50	0.17	0.0000
Aromatic flag[b]	−1.58	0.24	0.0000
Intercept[b]	0.08	0.12	0.4968

[a] See text. [b] Flag is Boolean type set to 1 if the criterion is matched.

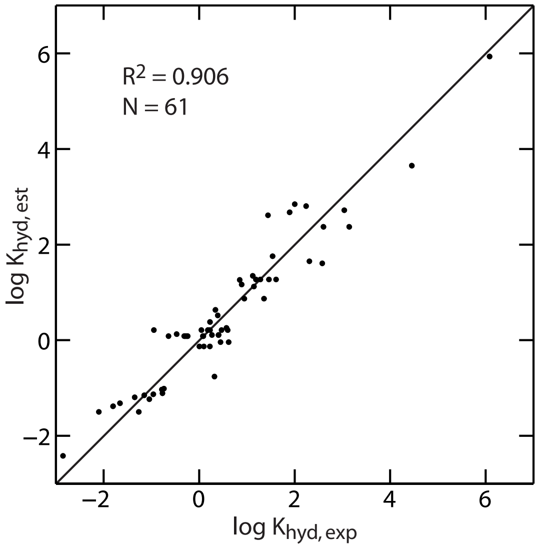

Fig. 1. Estimated hydration constant versus experimental values. The line is the y=x line.

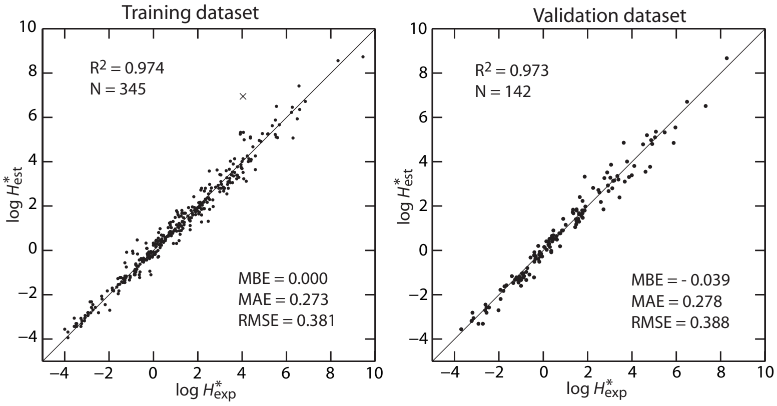

Fig. 2. Scatter plot of estimated logH^* using GROMHE versus experimental logH^* for the training set (left panel) and the validation set (right panel). The line is the y=x line. The (x) symbol represents oxo-acetic acid.

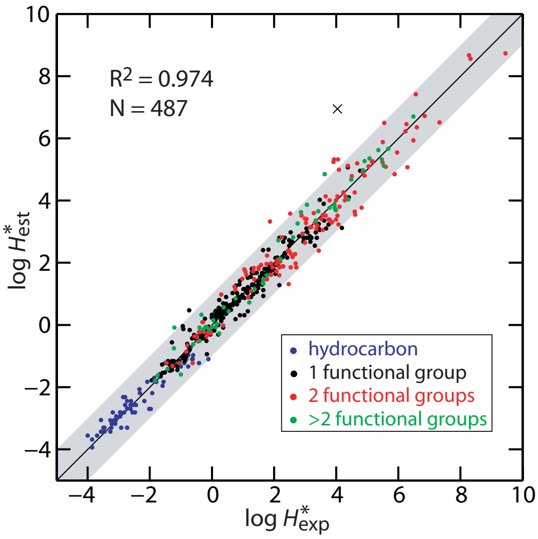

Fig. 3. Scatter plot of estimated versus experimental logH^* for the GROMHE method. The line is the y=x line and the grey area represents agreement within one log unit. The (x) symbol represents oxo-acetic acid.

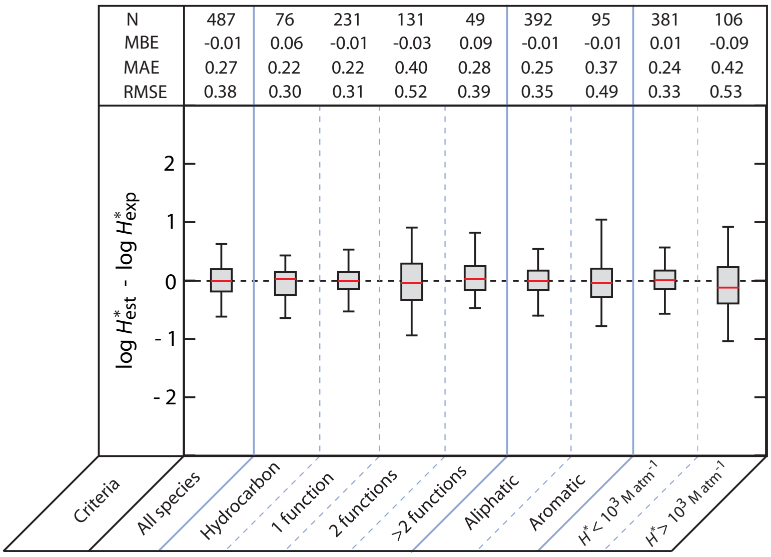

N	487	76	231	131	49	392	95	381	106
MBE	-0.01	0.06	-0.01	-0.03	0.09	-0.01	-0.01	0.01	-0.09
MAE	0.27	0.22	0.22	0.40	0.28	0.25	0.37	0.24	0.42
RMSE	0.38	0.30	0.31	0.52	0.39	0.35	0.49	0.33	0.53

Fig. 4. Mean bias error (MBE), mean absolute error (MAE), root mean square error (RMSE) and box plot for the error distribution in the estimated logH^* value with the GROMHE method. The whiskers of the box plot show the 5th and 95th percentiles, the box shows the second and third quartile and the red line gives the median value of the distribution.

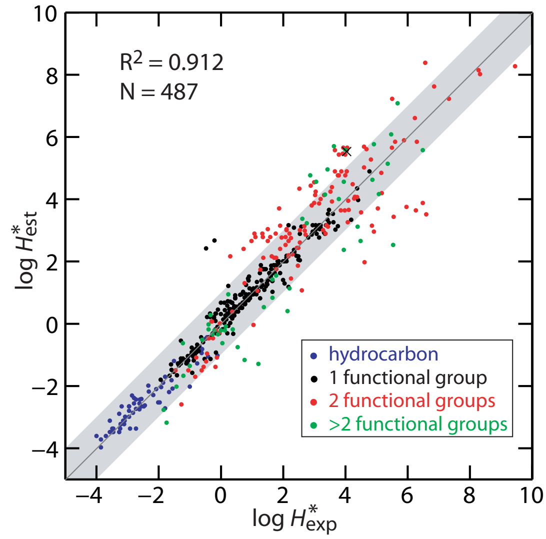

Fig. 5. Scatter plot of estimated versus experimental logH^* for the HWINb method. The line is the y=x line and the grey area represents agreement within one log unit. The (x) symbol represents oxo-acetic acid.

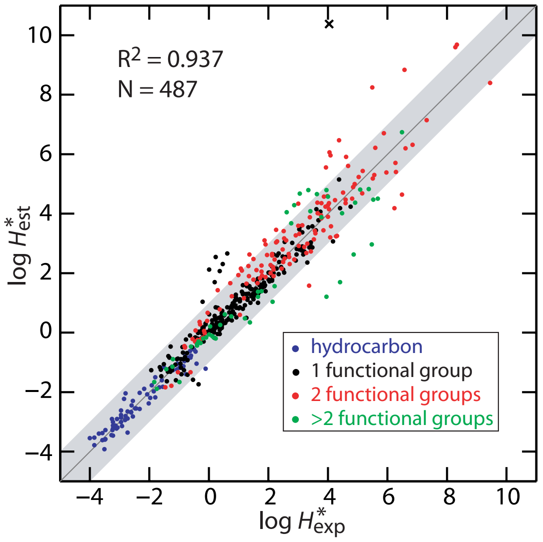

Fig. 6. Scatter plot of estimated versus experimental logH^* for the SPARC-v4.2 method. The line is the y=x line and the grey area represents agreement within one log unit. The (x) symbol represents oxo-acetic acid.

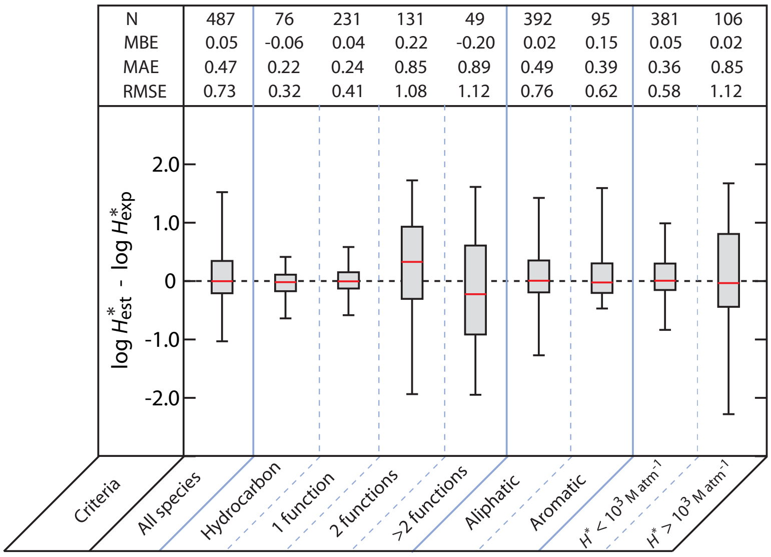

Criteria	All species	Hydrocarbon	1 function	2 functions	>2 functions	Aliphatic	Aromatic	$H^* < 10^3$ M atm^{-1}	$H^* > 10^3$ M atm^{-1}
N	487	76	231	131	49	392	95	381	106
MBE	0.05	-0.06	0.04	0.22	-0.20	0.02	0.15	0.05	0.02
MAE	0.47	0.22	0.24	0.85	0.89	0.49	0.39	0.36	0.85
RMSE	0.73	0.32	0.41	1.08	1.12	0.76	0.62	0.58	1.12

Fig. 7. Mean bias error (MBE), mean absolute error (MAE), root mean square error (RMSE) and box plot for the error distribution in the estimated logH^* value with the HWINb method. The whiskers of the box plot show the 5th and 95th percentiles, the box shows the second and third quartile and the red line gives the median value of the distribution.

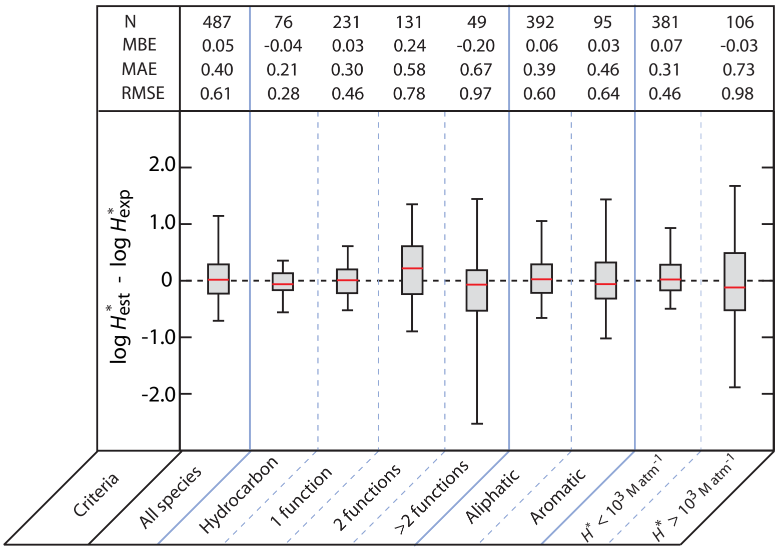

Criteria	All species	Hydrocarbon	1 function	2 functions	>2 functions	Aliphatic	Aromatic	$H^* < 10^3$ M atm^{-1}	$H^* > 10^3$ M atm^{-1}
N	487	76	231	131	49	392	95	381	106
MBE	0.05	-0.04	0.03	0.24	-0.20	0.06	0.03	0.07	-0.03
MAE	0.40	0.21	0.30	0.58	0.67	0.39	0.46	0.31	0.73
RMSE	0.61	0.28	0.46	0.78	0.97	0.60	0.64	0.46	0.98

Fig. 8. Mean bias error (MBE), mean absolute error (MAE), root mean square error (RMSE) and box plot for the error distribution in the estimated logH^* value with the SPARC-v4.2 method. The whiskers of the box plot show the 5th and 95th percentiles, the box shows the second and third quartile and the red line gives the median value of the distribution.